

KEYNOTE ARTICLE

From Solvolysis to Electron Transfer: Direct Observation of Ion-pair Dynamics by Time-resolved Spectroscopy

T. Michael Bockman and Jay K. Kochi

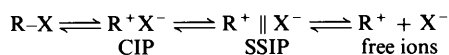
Chemistry Department, University of Houston, Houston, TX, 77204-5641 USA

Contents

- I. Historical Perspective
- II. Recent Advances in the Prompt Generation of Transient Ion Pairs by Laser-flash Techniques
 - A. Direct Photo-heterolysis
 - B. Electron-transfer Quenching
 - C. Charge-transfer Activation
- III. Microdynamics of Ion-pair Behaviour: Solvent and Salt Effects.
 - A. Internal Return and Solvent Separation *via* Picosecond Kinetics
 - B. External Return, Ion Dissociation and Reassociation *via* Nanosecond/Microsecond Kinetics
 - C. Special Salt Effects
- IV. Chemical Manifestations of Ion-pair Dynamics as Modified by Solvent Polarity and by Added Salt
 - A. Kinetics of Electron Transfer in Pyridinium/Carbonylmanganate Ion Pairs
 - B. Product Distribution on Aromatic Substitution. Trinitromethylation/Nitration of Anisoles
 - C. Photoinduced Dehydrosilylation/Alkylation of Enol Silyl Ethers
- V. Epilogue

I. Historical Perspective

The association of oppositely charged ions in solution has traditionally been addressed from two distinct points of view. Thus physical chemists have focussed on the *steady-state behaviour* of electrolytes at equilibrium, while physical organic chemists have conceived of the *dynamic behaviour* of ions as transient intermediates. The important distinction between the contact ion pair (CIP) and the solvent-separated ion pair (SSIP) was drawn simultaneously by Fuoss¹ and by Winstein² from these disparate points of view. Fuoss based his arguments on the thermodynamics of the coulombic interaction of ions, whereas Winstein based his on the kinetics of chemically reacting ion pairs. Nevertheless, both lines of argument yielded essentially the same picture of rapidly interconverting CIP and SSIP in equilibrium with free ions, as depicted in Scheme 1.



Scheme 1

In the following years, the application of a variety of spectroscopic techniques has verified the general formulations of Fuoss and Winstein.³ For the most part, such studies have concentrated on static (equilibrium) ion pairing. Infrared⁴ and electronic spectroscopy,⁵ magnetic resonance techniques,⁶ and ultrasonic relaxation⁷ have been used to probe ion pairing in aqueous and nonaqueous systems. For example, contact and solvent-separated ion pairs have been identified by changes in the absorption spectra of alkali metal/radical-anion salts.⁸ Infrared measurements have pinpointed structural changes attendant upon formation of the CIP,⁹ and the electronic interaction between cation and anion in the CIP has been probed by charge-transfer spectroscopy.^{10,11} The use of these

techniques has also extended the concept of ion association to include not only the simple ion pairing of cations and anions, but a wealth of aggregated species (triple ions, quadrupoles, and higher ionic clusters).¹² In the application of these various physicochemical techniques to studies of ion pairing, it is notable that the Winstein picture of contact and solvent-separated ion pairs as *transients*—that is, as reactive intermediates in chemical reactions—has somehow been obscured. This relative neglect generally stemmed from practical problems associated with the generation and observation of short-lived species at sufficiently high concentrations in chemical reactions far from equilibrium.¹³

The kinetics of the loss of optical activity in solvolytic systems established the lifetime of the contact ion pair to be very short.¹⁴ Thus internal return and solvent separation were temporally classified as picosecond and nanosecond processes. At the time that the CIP/SSIP dichotomy was first formulated (the mid-1950s), the direct observation of solvolytic intermediates was not possible. Later, in the mid-1960s, methods began to be developed for determining rate constants on these timescales, but these techniques were based on the observation of relaxation processes near equilibrium.^{15,16} Physical organic chemists studying transient ion pairs in solvolysis (and related reactions) continued to rely on overall reaction kinetics and product distributions, which provided merely ratios of rate constants.

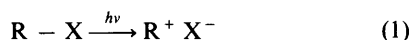
II. Recent Advances in the Prompt Generation of Transient Ion Pairs by Laser-flash Techniques

The development of laser-flash photolysis¹⁷⁻¹⁹ supplied the necessary tools to study chemical systems on the nanosecond and picosecond timescales relevant to ion-pair dynamics. The

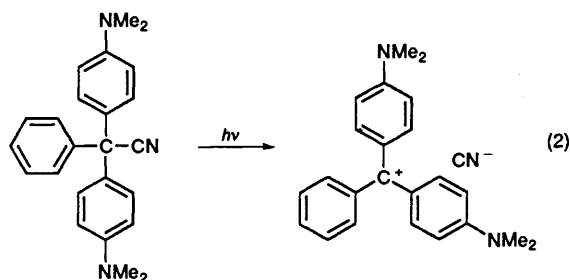
energy provided by the laser pulse was available for the generation of the reactive ion pair in either its contact or solvent-separated forms, and the kinetics of internal return, solvent separation, external return, and ionic dissociation/reassociation could then be observed directly by fast kinetic spectroscopy. The development of short-pulse lasers has spawned a variety of photochemical approaches, which differed in the precursor systems chosen to generate the ion pair.

A. Direct Photo-heterolysis

The most direct procedure for CIP generation was the laser-induced heterolysis of the R–X bond in Scheme 1, *i.e.*, eqn. (1) in



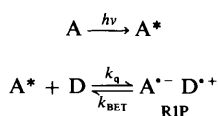
which X represents the anionic leaving group and R the cationic organic moiety. (It must be recognized, however, that the heterolysis must proceed *via* an excited state of the RX molecule.) This method has been particularly well exploited for triphenylmethyl halides and pseudohalides.^{20–22} For example, Spears *et al.* reported the picosecond photodissociation of malachite green leucocyanide (MG–CN) upon excitation at 300 nm.²¹ Manning and Peters assigned the initially formed



transient to the first excited singlet state of MG–CN.²² Full dissociation to the ion pair (MG⁺ CN[−]) occurred 3–5 ns following the laser excitation. Owing to the relatively long time needed for the formation of the contact ion pair, the kinetics of dissociation, solvent separation and the internal return could not be separately distinguished. Similarly, the photosolvolysis studies of McClelland and Steenken²³ addressed only reactions of *free* carbocations with anionic nucleophiles, since the photoionization process itself required several nanoseconds. Another drawback of the direct photogeneration of the CIP was the incursion of homolytic processes which frequently competed with ionization,²² particularly in less polar solvents. It is in these solvents that ion pairing is critical.

B. Electron-transfer Quenching

Ion pairs were also generated by electron-transfer quenching.²⁴ In this case, a photoexcited electron acceptor (A) reacted with a donor (D) to form the ion pair, Scheme 2.† [Note that the ion



Scheme 2

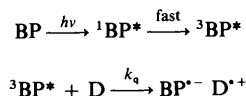
† It is equally possible to quench a photoexcited donor with the electron acceptor to generate the radical ion pair.²⁴

pair formed in this case is a *radical*-ion pair (RIP).] It was hoped that the subsequent competition between back electron transfer (k_{BET}) and ion-pair dissociation and reassociation could be observed by transient spectroscopy. This approach to the study of ion-pair dynamics was pioneered by Simon and Peters in a series of studies beginning in the early 1980s,²⁵ and contributions by Fessenden,²⁶ Mataga,²⁷ Haselbach,²⁸ Mattay²⁹ and others³⁰ have drawn upon this earlier work. The photoactivated acceptor most studied has been benzophenone.‡

A fundamental problem with the use of the quenching method to generate the ion pair in Scheme 2 was the requirement that the excited species encounter the quencher in order to form the RIP. The rate of ion-pair formation was thus limited to the rate of diffusive encounter in solution—typically *ca.* $10^{10} \text{ dm}^3 \text{ mol}^{-1} \text{ s}^{-1}$ in ordinary solvents.³² Thus for practical concentrations of quencher (*ca.* 1 mol dm^{-3}), the fastest reactions of the CIP which could be observed had lifetimes of the order of 100 ps. Finally, the initial state of the radical pair was not well defined in the quenching experiment, since both the SSIP and CIP could be formed by photoinduced electron transfer.²⁵

In addition to these fundamental problems with the quenching method, another complication arose from the spin multiplicity of the photogenerated ion pair. The ion pairs most studied were generated by the quenching of triplet acceptors, and the RIP was thus formed in its triplet state. However, triplet ion pairs must be reconverted into the singlet state prior to ion-pair return. As a result, triplet/singlet interconversion of the RIP must be included in a full description of the ion-pair dynamics.^{33,34} Despite the problems associated with the diversity of possible configurations (triplet or singlet, SSIP, CIP or free ions) and the uncertain starting point (SSIP, CIP or both) of the photogenerated ion pair, the desire to integrate electron transfer with ion-pair dynamics (Scheme 1) has made the photoinduced electron transfer in Scheme 2 the object of intense study.

Simon and Peters chose benzophenone (BP) as the sensitizer for various amine donors, particularly D = 1,4-diazabicyclo[2.2.2]octane (dabco), in their studies of ion-pair dynamics on the critical picosecond timescale.§²⁵ The picosecond kinetics were interpreted according to Scheme 3. The spectral blue shift



Scheme 3

of the BP^{•−} band maximum was attributed to the evolution of the initially formed SSIP [$\lambda_{\text{max}}(\text{BP}^{\cdot-}) = 715 \text{ nm}$] to the CIP [$\lambda_{\text{max}}(\text{BP}^{\cdot-}) = 690 \text{ nm}$] within 500 ps of excitation.¶ Unfortunately, these results were somewhat ambiguous, since it was not known whether the various CIPs and SSIPs could

‡ It should be noted that the radical ion pair in Scheme 2 does not recombine by bond formation between cation and anion (as in Scheme 1), but by back electron transfer. Although the intermediacy of the contact ion pair is required for bond formation, it is not necessarily required for back electron transfer,³¹ and so the identity of the ion pair (CIP or SSIP) in the various decay processes is ambiguous.

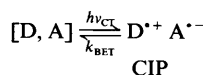
§ The radical anion, BP^{•−}, has been extensively used in (equilibrium) ion-pair studies, and spectral shifts of the visible absorption bands correlate with ion pairing of BP^{•−} with various alkali-metal cations.⁸ This behaviour raised the hope that the transient CIP and the SSIP might be spectrally distinguished.

¶ In the presence of Na⁺ ClO₄[−] the band shifted to 650 nm within 1.0 ns. This species was assigned to the Na⁺ BP^{•−} contact ion pair.

actually be distinguished.*†³⁵ At present, no conclusions regarding ion-pair dynamics, and, in particular, the dynamics of internal return and solvent separation, can yet be definitively drawn from studies of this complex and controversial system.‡

C. Charge-transfer Activation

Clearly, it is desirable to generate unequivocally the contact ion pair at early (picosecond) times. One successful approach utilized the intermolecular electron donor-acceptor (EDA) complex. Electron donors and acceptors react reversibly in solution to form EDA complexes, and these complexes possess unique charge-transfer (CT) absorption bands not found in the spectra of the separated donor and acceptor.§ Photostimulation of the CT bands ($h\nu_{CT}$) resulted in direct electron transfer to form the ion pair.³⁸ Since the CT bands only pertained to donors and acceptors in molecular contact, the ion pair so formed was the CIP (Scheme 4).



Scheme 4

No (local) excited-state species was an intermediate in this charge-transfer process, and the formation of the ion pair could be regarded as instantaneous. The major obstacle for the utilization of the radical CIP as generated by charge-transfer irradiation was the rapidity of the back electron-transfer process (k_{BET}) which commonly took place on timescales of 100 ps or less. Such short lifetimes for the CIP largely precluded solvent separation, and the spectral absorptions of the radical ions were generally observed to decay to the spectral baseline.¶

III. Microdynamics of Ion-pair Behaviour

The combination of charge-transfer activation and a fast follow-up reaction was the method of choice for generating contact ion

* In 1990, Davadoss and Fessenden repeated the transient experiments with BP and dabco in various solvents.²⁶ They observed a *red shift* (from 700 to 720 nm) of the band of $BP^{\cdot-}$ within 1.0 ns after excitation. This shift was attributed to the transformation from CIP to SSIP, the opposite process to that suggested by Peters. In 1993 Peters and Lee reported that upon repeating their experiment they observed *no* spectral band shift for $BP^{\cdot-}$ in the BP/dabco/MeCN system.³⁵

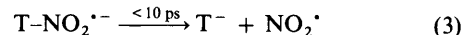
† The subsequent evolution of the $BP^{\cdot-}/dabco^{\cdot+}$ ion pair (whatever its status—CIP or SSIP) is also the subject of controversy. Contradicting earlier studies (on the nanosecond and microsecond timescales) Davadoss and Fessenden reported that $BP^{\cdot-}$ decays by first-order kinetics in all solvents.²⁶ They concluded that ion-pair separation does not occur. The validity of this conclusion was vigorously disputed by Haselbach *et al.*,²⁸ who reexamined the system on the nanosecond timescale and established that $BP^{\cdot-}$ decays by second-order kinetics in MeCN.

‡ Further complications in the BP-amine system were discovered by Mataga *et al.*³⁶ They showed that quenching of the singlet excited state of benzophenone ($^1BP^*$) by dabco and other amines makes a significant contribution to the production of ion pairs and to the picosecond decay processes. These workers also established the importance of the amine-BP electron donor-acceptor (EDA) complex, which was subject to laser excitation under the conditions of the experiments outlined above.

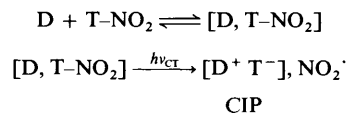
§ These absorption bands correspond to an electronic transition between the HOMO of the donor and the LUMO of the acceptor in the EDA complex.³⁷

¶ The kinetics of the back electron-transfer process in Scheme 4 are a subject of intense investigation at this time. In favourable cases, survival of the radical-ion pair until the ns/ μ s time regime is possible. See ref. 39.

pairs that exhibit the full range of ion-pair reactivity. If the acceptor in Scheme 4 was tetranitromethane (T-NO₂), the fast fragmentation of the acceptor radical anion (T-NO₂^{•-}) spontaneously yielded the anionic nucleophile trinitromethanide (T⁻) and nitrogen dioxide (NO₂[•]), eqn. (3).⁴⁰⁻⁴⁴ The



overall process was tantamount to the production of the contact ion pair [D⁺, T⁻] in a fast process without significant competition from back electron transfer processes, Scheme 5.



Scheme 5

Although the donor cation (D⁺) is a radical ion, which might be expected to combine rapidly with NO₂[•], this association was sufficiently slow^{||} that it did not materially interfere with the ps/ns dynamics of ion-pair recombination, separation and dissociation. (Since the ion-pair recombination of hydrocarbon cation radicals with nucleophiles was qualitatively indistinguishable from the more conventional carbenium ion/nucleophile combinations, the radical 'dot' is omitted from the donor cation, D⁺.)

Upon the charge-transfer irradiation of the EDA complexes of various 9-substituted anthracene donors (A) with T-NO₂, the characteristic bands of the anthracene cation radicals (A⁺ with λ_{max} ranging⁴⁵ from 680 to 770 nm) were observed. The trinitromethanide anion was identified as a spectral tail of its major absorption at $\lambda_{max} = 350$ nm.⁴⁰ Both transients formed within the laser pulse to indicate that the timescale for their formation was shorter than *ca.* 10 ps. Since this timescale was far faster than diffusive separation of the ions,⁴⁶ the anthracene cation and the trinitromethanide anion were generated as the CIP.

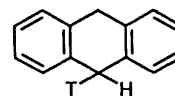
A. Internal Return and Solvent Separation via Picosecond Kinetics

The evolution of the CIPs formed from the various substituted anthracenes varied with the nature of the substituent on the 9-position and with the solvent.^{40,44} In nonpolar solvents (dichloromethane and hexane), the absorbances of the 9-nitro- and 9-cyano-anthracene cation radicals (N⁺ and C⁺) decayed to the spectral baseline within 2.5 ns after their generation with the laser pulse. Concurrently, the growth of new, additional transient species was observed with absorbances at $\lambda_{max} \approx 550$ nm, which were assigned to transitions of the covalent adducts (N-T and C-T).** Thus the process responsible for the decay of the anthracene cations (A⁺) and the formation of A-T was identified as the cation/anion annihilation (internal return), eqn. (4).



|| The radical-pair combination of NO₂[•] with D⁺ occurs on the microsecond timescale under conditions (polar solvent, added salt) in which ion-pair recombination is unimportant.⁴²

** The adducts have the dihydroanthracene structure, *i.e.*,



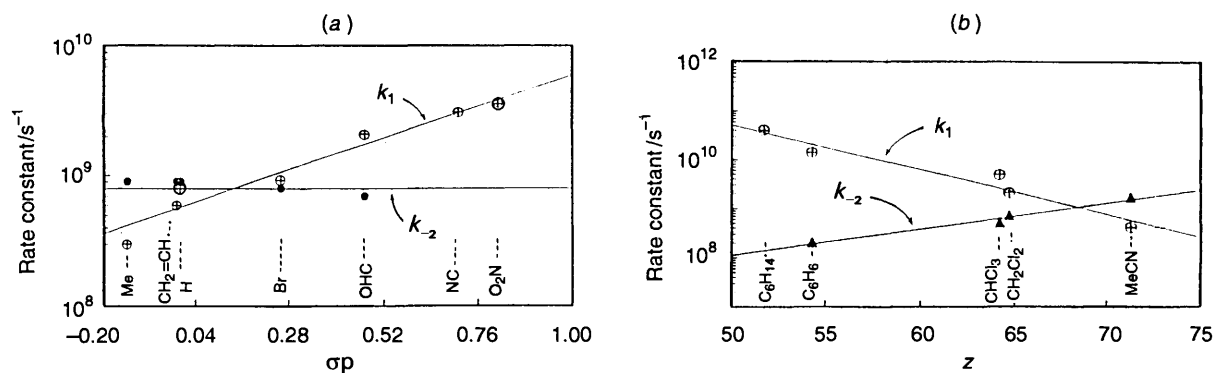


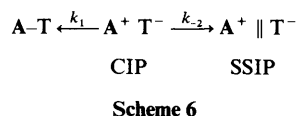
Fig. 1 (a) Effect of cation reactivity on the rate constants for internal return (k_1) and solvent separation (k_2) in dichloromethane; (b) effect of solvent polarity (Kosower Z value) on k_1 and k_2 for F^+

Table 1 Observed first-order picosecond rate constants and residuals for the decay of A^+ .^a

A^+ ^b	E_{red}^0 / V vs. SCE ^c	MeCN		CH_2Cl_2		C_6H_6	
		k_1^d	R^e	k_1^d	R^e	k_1^d	R^e
N^+	1.83	1.0	0.50	3.6	0	30	0
C^+	1.78	1.5	0.50	3.1	0	30	0
F^+	1.70	2.0	0.80	2.8	0.25	14	0
H^+	1.49	f	1.0	1.8	0.48	7.1	0
B^+	1.45	f	1.0	1.6	0.50	6.1	0
V^+	1.3	f	1.0	1.5	0.6	1.5	0.05

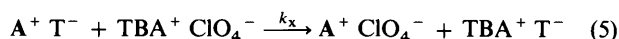
^a Generated as $A^+ T^-$ contact ion pairs by CT-irradiation of the EDA complex of the corresponding anthracene with tetranitromethane from Ref. 44. ^b Substituted anthracene cation radicals: N^+ (nitro), C^+ (cyano), F^+ (formyl), H^+ (unsubstituted), B^+ (bromo), and V^+ (vinyl). ^c Reduction potential of the anthracene cation, from ref. 45. ^d First-order rate constant at 23°C in units of $10^9 s^{-1}$. ^e Fraction of cation absorbance (relative to the initial amount) remaining after 2.5 ns. ^f No decay observed.

The absorption bands of the cations derived from 9-formyl-, 9-methyl- and 9-vinyl-anthracene (F^+ , M^+ and V^+) and from anthracene itself (H^+) did not return to the baseline within the 2.5 ns interval. Instead, the absorbance due to these cations decayed to a residual value within 2.5 ns, and it then persisted unchanged for the remainder of the 5 ns interval of observation. [The value of these residuals is listed in Table 1 as $R = A_{2.5 ns} / A_{max}$ where $A_{2.5 ns}$ is the absorbance of A^+ at λ_{max} 2.5 ns following the laser pulse, and A_{max} is the maximum value of the absorbance observed during the spectral evolution.] This behaviour pointed to the existence of a process, competitive with internal return, which effectively preserved the cation and anion from annihilation. Since the residual, R , increased with cation stability in the order: $R(N^+) = R(C^+) = 0$ and $R(F^+) < R(H^+) < R(V^+) < R(M^+)$ and with solvent polarity (acetonitrile > dichloromethane > benzene), it was ascribed to the competition from solvent separation of the contact ion pair, as formulated in Scheme 6.



Analysis of the decay kinetics by nonlinear regression techniques allowed the extraction of the rate constants k_1 for internal return and k_2 for solvent separation in Scheme 6. The variations in k_1 and k_2 with cation stability (Hammett σ_p for the 9-substituent)⁴⁷ and solvent polarity (Kosower Z-value)^{10a} are shown in Fig. 1. Not surprisingly, the remote substituent

exerted no effect on the purely physical process of solvent separation (horizontal line for k_2 in the Hammett plot). On the other hand, the increased reactivity of cations that contain electron-withdrawing substituents was reflected in their increased rates of internal return ($\rho_{IR} = +1.0$). Solvent polarity exerted an effect on both processes—with k_1 decreasing and k_2 increasing with enhanced solvent polarity (higher Z).^{*} The combination of these factors which controlled the relative magnitude of k_1 and k_2 led to (a) exclusive internal return in benzene, (b) exclusive solvent separation in acetonitrile (for all but the most reactive cations), and (c) competitive internal return and solvent separation in chloroform and dichloromethane. A distinct increase in the residual, R , was noted as the concentration of added salt (tetra-*n*-butylammonium perchlorate, $TBA^+ ClO_4^-$) was increased from 0 to 0.1 mol dm^{-3} .⁴⁴ This effect was assigned to the dissociation of the CIP by ion-pair exchange, eqn. (5).

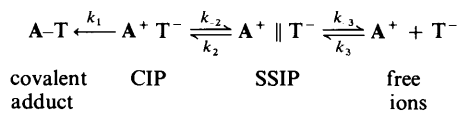


B. External Return, Ion Dissociation and Reassociation via Nanosecond/Microsecond Kinetics

The values of the residual ($R \approx 0.5$ in Table 1) for the cations F^+ , H^+ , B^+ and V^+ in dichloromethane indicated a rough balance between the rates of ion-pair separation and annihilation. Accordingly, ion-pair dynamics in this solvent were made the subject of further study.⁴⁰ Careful analysis of the picosecond decay kinetics showed a negligible contribution on this timescale for external ion-pair return (SSIP \rightarrow CIP \rightarrow covalent adduct).⁴⁴ For this reason, the slower kinetics of this process were examined on the longer nanosecond and microsecond timescales.

The decay profiles for the cations (H^+ , B^+ , V^+ and 9-phenylanthracene cation, P^+) in dichloromethane were biphasic. First-order decays ($k_{obs} \approx 1-3 \times 10^7 s^{-1}$) prevailed on timescales less than 200 ns, but the subsequent decay of the cation radicals on the microsecond timescale proceeded by second-order kinetics. The product formed from the cation radicals was identified spectrally as the covalent adduct, A-T. Accordingly, the first-order and second-order phases of the spectral decay of these cations could be identified with the processes of external ion-pair return (k_2) and external ion return (k_3), respectively, in Scheme 7.

* The decrease in k_1 relates to the decrease of the free energy of ion pairs in solvents of increasing polarity. The coulombic contribution is given by $\Delta G_C = e^2/r\epsilon$ where r is the interionic distance and ϵ is the relative permittivity of the solvent.



Scheme 7

Moreover, the rate of ion-pair dissociation (k_{-3}) could be calculated from the fraction of cations subject to the second-order decay process (the free ions in Scheme 7). Thus the full quantitative expression of the Winstein mechanism was achieved. The values of *all* of the pertinent rate constants, as obtained by time-resolved kinetic spectroscopy on three timescales, are summarized in Tables 2 and 3. These results were uncomplicated by spin dynamics, excited states, ambiguity about the initial state of the ion pair or electron-transfer processes for ion-pair annihilation.

C. Special Salt Effects

The use of salt effects played a critical role in the development of the solvolysis mechanism in Scheme 7.⁴⁰ Thus the addition of small quantities ($< 5 \times 10^{-3}$ mol dm⁻³) of tetra-*n*-butylammonium perchlorate (TBA⁺ ClO₄⁻) as an 'innocent' salt completely eliminated the first-order phase of the decay kinetics, and a uniform second-order decay of A⁺ was observed over the entire ns/ μ s timescale. The observed rate constants for this

Table 2 Rate constants for internal return and solvent separation of [A⁺ T⁻] contact ion pairs^a

A ⁺ b	CH ₂ Cl ₂		C ₆ H ₆	
	k ₁ ^c	k ₋₂ ^d	k ₁ ^c	k ₋₂ ^d
F ⁺	2.1	0.70	14	0.2
H ⁺	1.8	0.48	7.1	—
B ⁺	1.6	0.5	6.1	—
V ⁺	1.5	0.6	1.5	0.05

^a Obtained by nonlinear-regression analysis of k₁ and R in Table 1.

^b Anthracene radical cations as in Table 1. First-order rate constants for ^c internal return and ^d solvent separation in units of 10⁹ s⁻¹.

Table 3 Rate constants for external ion-pair return, ion dissociation and ion reassociation for anthracene cation/trinitromethanide ion pairs^a

A ⁺ b	k ₂ /10 ⁷ s ⁻¹ c	k ₋₃ /10 ⁶ s ⁻¹ d	k ₃ /10 ¹¹ dm ³ mol ⁻¹ s ⁻¹ e
H ⁺	4.3	4.6	2.0
B ⁺	4.6	6.9	2.0
V ⁺	2.1	5.8	2.0
P ⁺	3.9	5.7	2.0

^a Generated by the 10 ns 532 nm laser excitation of the [A, T-NO₂] EDA complex in dichloromethane. ^b Anthracene cation radicals as in Tables 1 and 2. Rate constants for ^c external ion-pair return, ^d ion dissociation and ^e ion reassociation (external ion return) in Scheme 7.

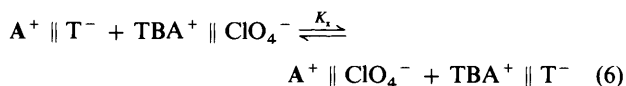
Table 4 Salt effects on the decay kinetics of anthracene cations^a

A ⁺	log (k _{obs} /A ⁻¹ s ⁻¹) ^b	log (k _{obs} /A ⁻¹ s ⁻¹) ^c	log (k _{obs} /A ⁻¹ s ⁻¹) ^d	log (k _{obs} /s ⁻¹) ^e	log (k _{obs} /s ⁻¹) ^f
H ⁺	7.6	5.4	5.6	7.46	7.43
B ⁺	7.5	5.5	5.5	7.43	7.44
V ⁺	7.57	5.5	5.3	6.99	7.04
P ⁺	7.64	5.5	5.7	7.15	7.23

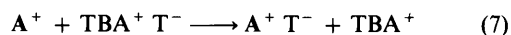
^a Generated as the [A⁺ T⁻] contact ion pairs by 532 nm laser photolysis of the EDA complex of A with tetranitromethane in dichloromethane.

^b Observed second-order rate constant (in absorbance units) for the decay of A⁺ on the microsecond timescale in the absence of added salt. ^c Second-order rate constant in the presence of 0.1 mol dm⁻³ TBA⁺ ClO₄⁻. ^d Second-order rate constant in acetonitrile. ^e First-order rate constant for disappearance of A⁺ in the presence of 0.01 mol dm⁻³ TBA⁺ C(NO₂)₃⁻. ^f Rate constant for (initial) first-order decay of A⁺ on the nanosecond timescale.

second-order decay were identical with those determined in the polar solvent, acetonitrile. [Compare columns 3 and 4 in Table 4.] This suppression of external return by small concentrations of added salt accorded precisely with Winstein's formulation of the *special salt effect*,⁴⁷ which operates by separation of the reactive SSIP, A⁺ || T⁻, via the ion-exchange process,* viz. eqn. (6).



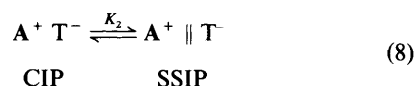
The addition of the trinitromethanide anion (common salt) as the tetra-*n*-butylammonium salt (TBA⁺ T⁻) altered the kinetics of cation decay to *first order* over the *entire* ns/ μ s timescale. Common salt thus diverted the ion dissociation process, by converting all the free ions into contact ion pairs, eqn. (7).



Accordingly, the pseudo-first-order rate constant for cation decay in the presence of TBA⁺ T⁻ was *exactly* equal to the rate constant for the first-order *phase* of the decays obtained (on the ns timescale) in the absence of added salt. [See columns 5 and 6 in Table 4].

Moderately reactive cations, such as H⁺, P⁺, B⁺ and V⁺, obeyed the decay kinetics that showed the full range of ion-pair behaviour only in dichloromethane. Thus in benzene, the decays of these cations followed first-order kinetics to indicate the unimportance of ion-pair dissociation in nonpolar media.⁴⁹ In contrast, the decays of the various anthracene cations in acetonitrile followed second-order kinetics throughout the ns/ μ s timescale. Combined with values of the residual absorption (R, which are essentially equal to unity in Table 1), this observation indicated that free ions were the dominant species in ion-pair annihilation reactions in acetonitrile.

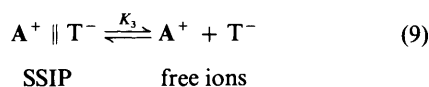
In dichloromethane, the thermodynamics favour the SSIP. Thus K₂ in eqn. (8) [as calculated from the rate constants in



Tables 2 and 3; K₂ = k₋₂/k₂] was about 10, which represented about 1.5 kcal mol⁻¹ of free energy that favoured the SSIP over the CIP. The corresponding equilibrium for solvent separation,

* Since the concentration of reactive ion pairs (as generated either by photolysis or in the thermal solvolysis reaction) is very small, the addition of even millimolar quantities of innocent salt is sufficient to convert all of the active ion pairs into the inactive forms. The inactive ion pairs, A⁺ || ClO₄⁻ and TBA⁺ || T⁻ behave, in effect, like free ions, and decay by second-order kinetics. Compare refs. 40 and 48.

K_3 , *i.e.*, eqn. (9) was of the order of $2-3 \times 10^{-5} \text{ mol dm}^{-3}$. This



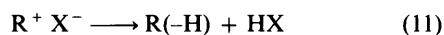
value compared favourably with the ion-pairing equilibrium constant, $K_3 \approx 10^{-5} \text{ mol dm}^{-3}$, previously found for large ions in dichloromethane.¹¹ The use of kinetic methods for elucidating the *thermodynamics* of ion pairing thus provided an adjunct to recent studies on the thermodynamics of the ionization step ($\text{RX} \rightarrow \text{CIP}$) itself.⁵⁰⁻⁵²

IV. Chemical Manifestations of Ion-pair Dynamics as Modified by Solvent Polarity and Added Salt

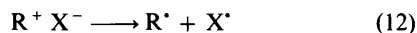
As originally formulated,^{2,47,48} internal return signified the (re)formation of the R-X bond in the solvolytic mechanism in Scheme 1. Polar solvents and added salt, by dissociation of the CIP and SSIP, accelerated the net rate of R-X bond heterolysis.⁵³⁻⁵⁵ However, the application of the kinetic formulation in Scheme 1 is not restricted to cases in which internal return simply regenerated the starting material. *Any reaction of the ion pair which annihilates the opposed charges is the functional equivalent of internal return.* Such ion-pair annihilation reactions can include bond formation, eqn. (10), as



manifested in the classical solvolysis mechanism, and also in the collapse of the anthracene-derived $[\text{A}^+ \text{T}^-]$ contact ion pair described in Section III. *Proton transfer* reactions also serve to annihilate charges, eqn. (11). Here R(-H) signifies the alkene or

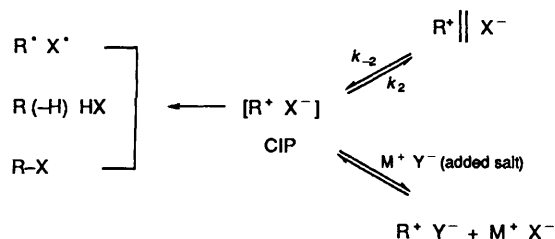


other product of the deprotonated cation. Finally, considerable attention has been directed to *electron-transfer* reactions, which are another means for the destruction of the ion pair, eqn. (12).



Regardless of the mode of ion-pair return, the expressions for the various reactions of the ion pair, *i.e.*, ion return, solvent separation, dissociation and reassociation, are identical. We thus expect the effects of solvent and added salt, as delineated by the time-resolved spectroscopic investigation described above, to apply to all three types of ion-pair annihilations.

There are two principal chemical consequences of the various ion-pair transformations on these internal return processes. For the simplest case, in which internal return represents the only mode of reaction of the ion pair, polar solvents and added salts will exert an effect on the *kinetics* of the ion-pair annihilation. Such a situation is illustrated in Scheme 8a. Disassembly of the

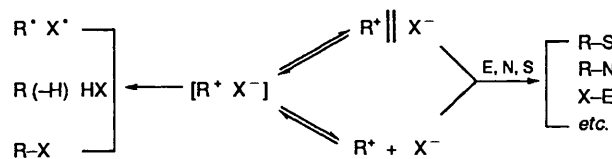


Scheme 8a

contact ion pair (by solvent separation and the special salt effect) depletes the concentration of this critical intermediate,

and results in a decreased rate for the various internal return processes.

Suppose, however, that the reactions of the cation (R^+) or the anion (X^-) are *not* confined to internal return processes. The ions may react, for example, with the solvent or with neutral nucleophiles or electrophiles. These scavenging reactions *compete* with internal return, as illustrated in Scheme 8b, where



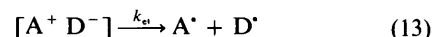
Scheme 8b

E, N and S represent the scavenging electrophile and nucleophile, and the solvent. In this case, polar solvents and added salt promote those reactions which compete with internal return. Very dramatic salt and solvent effects may then be observed on the *distribution of the reaction products*.^{*} In the remainder of this article, we will illustrate these two facets of ion-pair dynamics as applied to internal return processes of (A) Electron transfer within organometallic ion pairs, (B) Bond formation in aromatic substitutions, and (C) Proton transfer within photogenerated ion pairs.

Accordingly, in Part (A), we examine the purely kinetic effects expected for the uncomplicated internal return in Scheme 8a. In Parts (B) and (C), the unusual salt and solvent effects on product distributions which prevail in Scheme 8b will be explored.

A. Kinetics of Electron Transfer in Pyridinium/Carbonylmanganate Ion Pairs

The electron transfer (ET) from anionic donor (D^-) to cationic acceptor (A^+) is the simplest and most fundamental example of charge annihilation, eqn. (13). As such, interionic ET constitutes



an internal return process, and its kinetics are governed by the formation and disassembly of the $[\text{A}^+ \text{D}^-]$ contact ion pair. The rate of the overall reaction is thus subject to the influence of solvent polarity and added salt as illustrated in Scheme 8a.

For the study of the solvent and salt effects on the electron-transfer process in eqn. (13), the carbonylmanganate anion,⁵⁶ $\text{Mn}(\text{CO})_5^-$, served as a suitable anionic donor, D^- , owing to its low one-electron oxidation potential⁵⁷ of $E_{\text{ox}}^{\circ} = -0.11$ (*vs.* the standard calomel electrode, SCE). A series of *N*-methylpyridinium ions (Py^+)⁵⁸ were chosen as cationic acceptors (A^+). One equivalent of *N*-methylacridinium trifluoromethanesulfonate ($\text{Ac}^+ \text{OTf}^-$) was added to a solution ($0.010 \text{ mol dm}^{-3}$) of $\text{PPN}^+ \text{Mn}(\text{CO})_5^-$.[†] The infrared spectrum of the tetrahydrofuran solution showed the complete disappearance of the diagnostic carbonyl bands⁵⁹ of $\text{Mn}(\text{CO})_5^-$ and their replacement by the characteristic ν_{CO} bands of $\text{Mn}_2(\text{CO})_{10}$.⁶⁰ The presence of the dimeric *N,N'*-dimethyl-9,9'-biacridanyl (Ac-Ac) was indicated by its characteristic ¹H

^{*} Such a mechanistic dichotomy is analogous to the competition between cage and escape reactions of geminate radical pairs,^{33,34} but in that case, there is no control comparable to that exerted by solvent and added salt in the collapse and escape reactions of ions.

[†] PPN^+ is the bis(triphenylphosphoranyl)ammonium cation. The trifluoromethanesulfonate anion (OTf^-) is referred to as triflate hereafter.

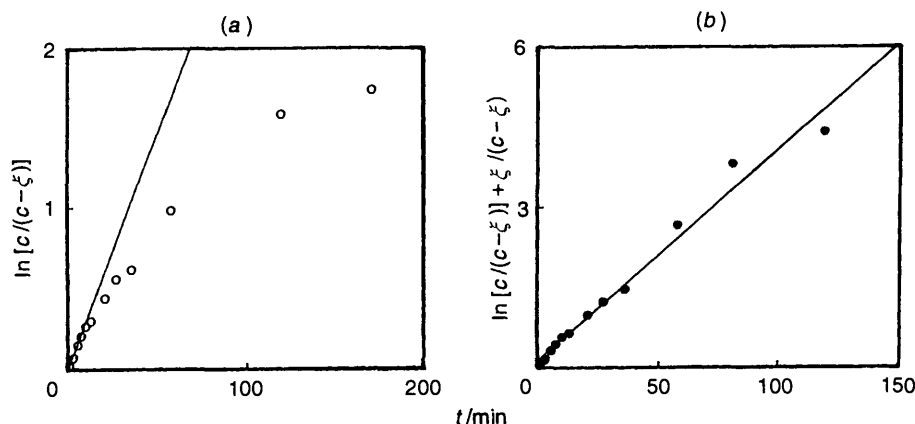


Fig. 2 Progress of the annihilation of *N*-methyl-3-cyanopyridinium/ $\text{Mn}(\text{CO})_5^-$ ion pairs fitted to (a) first-order kinetics and (b) kinetics in Scheme 9

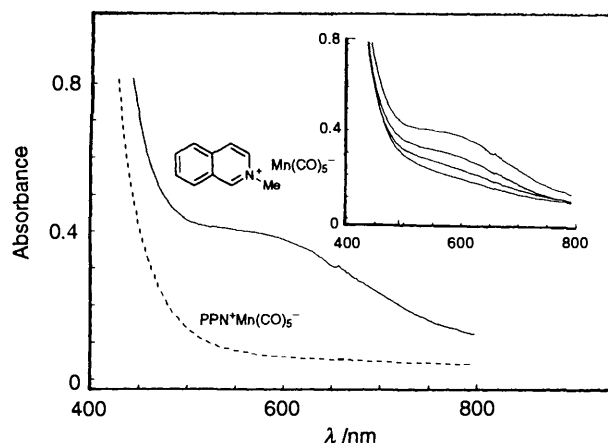
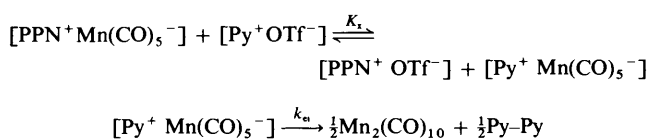


Fig. 3 Charge-transfer absorption spectrum of *N*-methylisoquinolinium/ $\text{Mn}(\text{CO})_5^-$ in tetrahydrofuran. The dashed line is the cut-off of the carbonylmanganate anion (as the PPN^+ salt). The inset shows the decrease of the CT band upon addition of one, two and four equivalents of inert salt ($\text{TBA}^+ \text{ClO}_4^-$)



Scheme 9

led to the integrated rate expressions given in eqn. (19), in which

$$\ln [c/(c - \xi)] + [\xi/(c - \xi)] = k_{et} t \quad (19)$$

c is the initial (equimolar) concentration of both the pyridinium and the manganate salts and ξ is the extent of reaction. [See the Appendix for a derivation of the rate expressions.] A plot of the extent of reaction, fitted to this equation is shown in Fig. 2(b). This kinetic equation was used to determine the rate constants for the less reactive cations in Table 5 (*i.e.*, those with $\tau_{\frac{1}{2}} > 10$ min). Two points should be noted about the rate law in eqn. (19). (1) This expression yielded directly the first-order rate constant for internal return *via* electron transfer, *i.e.*, k_{et} in Scheme 9. (2) As shown in the Appendix, the expression reduced to the rate law for first-order kinetics, with the observed rate constant $\frac{1}{2}k_{et}$ during the first half-life of the reaction.

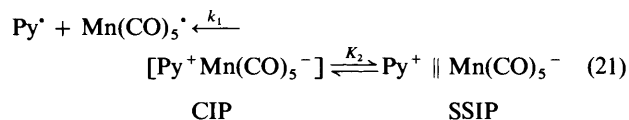
The rate law for the reaction in the presence of added salt (at a concentration of c_s) is given by the modified expression, eqn. (20). High concentrations of added salt increased the magnitude

of the second term in eq. (20), and thereby increased the half-life of the reaction.* This equation represents the quantitative

$$\ln [c/(c + \xi)] + [(c + c_s)/c][\xi/(c - \xi)] = k_{et} t \quad (20)$$

expression of the special salt effect and was used to determine k_{et} for the highly reactive salts in Table 5.

The kinetics of the decay of the $[\text{Py}^+ \text{Mn}(\text{CO})_5^-]$ contact ion pair identified the role of solvent and added salt in the dissociation of the contact ion pair and the circumvention of internal return. *Polar solvents* separated the ions. This process could be pinpointed by the disappearance of the CT band of the contact ion pair in acetonitrile. The decreased rate of the internal return step (electron transfer) thus follows from this preequilibrium, *i.e.*, eqn. (21) (compare Scheme 6) where k_1

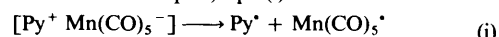


($=k_{et}$) and K_2 represent the rate constant for internal return and equilibrium constant for SSIP formation, respectively.

For the carbonylmanganate ion pairs, the effect of *added salt* on the dissociation of the CIP was manifested in three different ways: (i) the diminution of the CT band of $[\text{Py}^+ \text{Mn}(\text{CO})_5^-]$, (ii) the reduced rate of the electron transfer in eqn. (14), and (iii) the form of the rate law in eqn. (19).† All three effects stem from the ion-pair exchange, induced by added salt, in Scheme 9. The role of added salt in the depletion of the 'active' ion pair, $[\text{Py}^+ \text{Mn}(\text{CO})_5^-]$ was clear from the diminution of the CT band in Fig. 3. Thus the effects of solvent and added salt on the *electron*

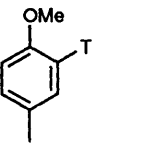
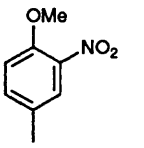
* No (normal) effect⁶⁶ of added salt on k_{et} was assumed.

† The unusual form of the rate law for ion-pair collapse is a manifestation of the fact that an equivalent of added inert salt ($\text{PPN}^+ \text{OTf}^-$) is present in the reaction mixture, owing to the introduction of the pyridinium cation and manganate anion as the triflate and PPN^+ salts, respectively. Qualitatively, it can be understood that at the commencement of the reaction, the kinetics are dominated by the first-order collapse of the 'active' ion pair, eqn. (i).



As the reaction proceeds, fewer and fewer 'active' ion pairs are present and most of the Py^+ and $\text{Mn}(\text{CO})_5^-$ ions are paired with OTf^- and PPN^+ , respectively. The CT band, which reflects the concentration of reactive ion pairs, vanishes and the overall reaction becomes sluggish. This kinetics behaviour has its counterpart to the overall second-order decays of the anthracene cation observed in the presence of added innocent salt. [See section III B.] Indeed, the kinetic expression in eqn. (20) can be shown to reduce to second-order kinetics in the presence of a large excess of added salt (see the Appendix).

Table 6 Solvent and salt effects on charge-transfer substitution^a

Solvent	Added salt	Alkylation (%)	Nitration (%)
			
CH ₂ Cl ₂	—	95	5
	TBA ⁺ ClO ₄ ^{-b}	0	100 ^c
	TBA ⁺ T ^{-d}	76	24 ^c
MeCN	—	5	95 ^c
	TBA ⁺ ClO ₄ ^{-b}	0	100 ^c
	TBA ⁺ T ^{-d}	10	90 ^c
C ₆ H ₆	—	85	15
	TBA ⁺ ClO ₄ ^{-b}	75	25
	TBA ⁺ T ^{-d}	100	0

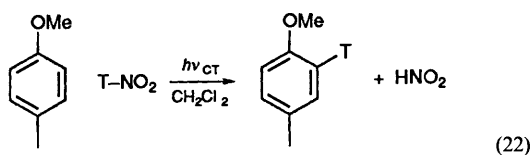
^a Formed by CT irradiation of the EDA complex formed from 4-methoxytoluene (0.06 mol dm⁻³) and tetranitromethane (0.8–1.7 mol dm⁻³). From ref. 42(a). ^b Tetra-*n*-butylammonium perchlorate (0.2 mol dm⁻³). ^c Including minor amounts (< 30%) of 4-methyl-2-nitrophenol. ^d Tetra-*n*-butylammonium trinitromethanide (0.01 mol dm⁻³).

transfer kinetics of ion pair annihilation was found to be essentially the same as the effects on the ion-pair collapse of the anthracene-derived CIPs, despite the enormous difference in timescale (hours *vs.* picoseconds) for the two reactions.

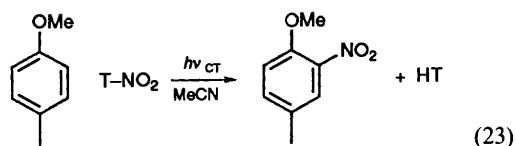
B. Product Distributions in Aromatic Substitution.

Trinitromethylation/Nitration of Anisoles

Like the anthracenes described in Section III, anisoles are electron donors.⁶⁷ As such they readily formed coloured EDA complexes upon their exposure to tetranitromethane (T-NO₂).^{42,68} Upon the CT irradiation of these complexes, the colours were bleached and substituted anisole derivatives were obtained in high yield. The distribution of these products varied dramatically with solvent polarity and the presence or absence of added salt. The solvent and salt effects were particularly marked for the donor 4-methoxytoluene (MA).⁴² Thus the charge-transfer irradiation of the EDA complex of methoxytoluene and tetranitromethane dissolved in *dichloromethane* or *benzene* yielded the product of aromatic *trinitromethylation* (alkylation), together with one equivalent of nitrous acid, eqn. (22).



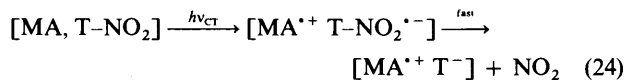
On the other hand, the replacement of the nonpolar solvents with *acetonitrile* resulted in predominant *nitration*, eqn. (23).



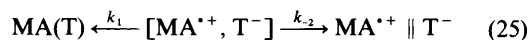
[One equivalent of nitroform was formed with the nitrated anisole.] The same changeover from alkylation to nitration could be effected by the addition of inert salt. Thus the addition of tetra-*n*-butylammonium perchlorate (TBA⁺ ClO₄⁻) efficiently diverted the course of the reaction (in dichloromethane)

from predominant trinitromethylation to predominant nitration.⁴² Table 6 shows the distinct effects of solvent and added salt in altering this distribution of the substitution products.

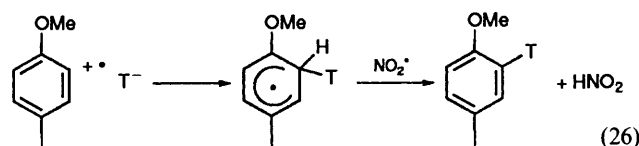
The explanation for these solvent and salt effects lay in the dynamics of the photogenerated [MA^{•+} T⁻] ion pair. Time-resolved spectroscopy showed that the first step of the reaction sequence was the formation of this ion pair, accompanied by one equivalent of nitrogen dioxide (NO₂), eqn. (24). This



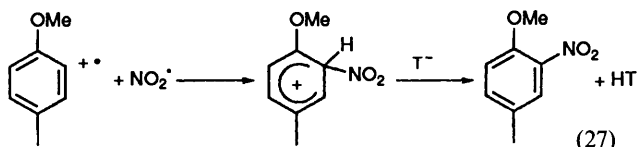
reaction was identical with the dissociative electron transfer which produced the [A⁺, T⁻] ion pairs in Section III. The reaction mechanism could thus be resolved, by analogy, into a competition between ion-pair annihilation *via* bond formation and solvent separation, *i.e.*, eqn. (25). [Compare Scheme 6.] The



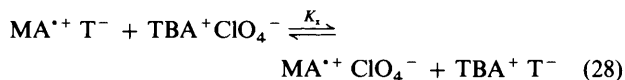
covalent adduct, MA(T), was the immediate precursor to the trinitromethylation product,⁴² eqn. (26). The nitrogen dioxide



formed in the initial cleavage of TNO₂^{•-} scavenged the free MA^{•+} to form the nitration product *via* the σ -adduct or Wheland intermediate,^{42,69,70} eqn. (27).



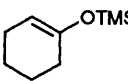
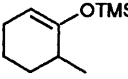
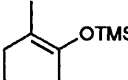
The competition between the ion-pair collapse of [MA^{•+} T⁻] in eqn. (26) and the radical-pair reaction of MA^{•+} with NO₂ in eqn. (27) defined the requisite conditions for the operation of solvent and salt effects on the distribution of products. Polar solvents such as acetonitrile facilitated solvent separation and ionic dissociation. The free cation radical thus formed reacted with the (uncharged) NO₂ with minimal interference from ion-pair collapse, and nitration predominated. The extensive degree of ion pairing which prevailed in dichloromethane and benzene facilitated internal return (*via* the bond-forming collapse reaction) to form the trinitromethylated product. These competing ionic pathways are generalized in Scheme 10 (ArH = MA). Added salt dissociated the ion pairs, eqn. (28).



Disassembly of the ion pair in eqn. (28) obviated the collapse of [MA^{•+} T⁻] and thus had the same effect on the product distribution as the solvent separation by acetonitrile.

This explanation for the solvent and salt effects in Table 6 was confirmed by the direct examination of the kinetics for the disappearance of MA^{•+} on the nanosecond/microsecond time-scale.⁴² In *benzene*, the disappearance of the cation radical was first order, which was identified in Section IIIB as a characteristic kinetic feature of ion-pair return. Addition of the

Table 7 Rate constants for electron-transfer quenching of chloranil triplet by donors

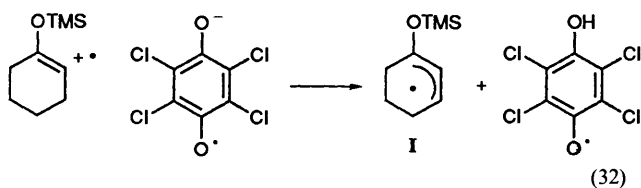
Donor	E_i/eV	Solvent	$k_q/10^9 \text{ dm}^3 \text{ mol}^{-1} \text{ s}^{-1}{}^a$
	8.3 ^b	CH ₂ Cl ₂ CH ₃ CN	10.0 5.9
	8.3 ^b	CH ₂ Cl ₂	8.8
	7.9 ^b	CH ₂ Cl ₂	9.0
Naphthalene	8.15 ^c	<i>n</i> -C ₃ H ₇ CN	7.0 ^d
Indole		CH ₃ CN	13 ^e
Styrene	8.5 ^c	CH ₃ CN	8.0 ^f

^a Rate constant for electron transfer from the donor to ³CA*, obtained from the pseudo-first-order decay of the absorbance at 510 nm. Ionization potentials from ^b ref. 78(a) and ^c ref. 78(b). Quenching rate constants from refs. ^d 79, ^e 78(c) and ^f 78(d).

spectroscopy established that in the presence of CTE ³CA* decayed completely 1.0 ns following the laser pulse. The anion radical, CA^{•-}, was the product in either solvent. Moreover, the rate constant k_q for quenching in Table 7 was essentially the same in both acetonitrile or dichloromethane with $k_q \approx 10^{10} \text{ dm}^3 \text{ mol}^{-1} \text{ s}^{-1}$ to indicate an essentially diffusion-controlled⁸⁶ electron transfer from CTE to ³CA*, eqn. (31).†



The process responsible for the decay of CA^{•-} and the formation of CAH[•] on the early nanosecond (1–3 ns) timescale can thus be ascribed to the deprotonation of CTE^{•+} to yield the allylic radical, I, eqn. (32). On account of the triplet spin state³⁹



of the RIP in eqn. (31), other internal return processes (bond formation and electron transfer) cannot occur. Thus the proton transfer in eqn. (32) is identified as critical charge-annihilation process taking place within the [CTE^{•+} CA^{•-}] contact ion pair.

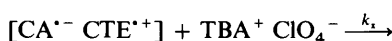
Because solvent separation is rapid and efficient in *acetonitrile* (see Section IIIA), the contact ion pair, [CA^{•-} CTE^{•+}], separated within the first few nanoseconds following its formation. Accordingly, CA^{•-} was observed to persist for microseconds. In *dichloromethane*, proton transfer was faster

† Identical UV and visible absorption bands were observed upon photostimulation of chloranil in the presence of 0.05 mol dm⁻³ cyclohexa-1,3-diene, which is a known source of CAH[•].^{81b} The possibility that the transient absorption bands belonged to the trimethylsilyl-substituted semiquinone radical (CA-TMS[•]) were ruled out by independent generation of CA-TMS[•]. Chloranil was photolysed in the presence of 0.05 mol dm⁻³ hexamethyldisilane in dichloromethane solvent.⁸⁷ A transient was observed with two maxima, at 435 and 340 nm. The UV band of this transient clearly differed from the UV band of authentic CAH[•].

than solvent separation, and only CAH[•] persisted to the ns/μs timescale (Scheme 11).

**Scheme 11**

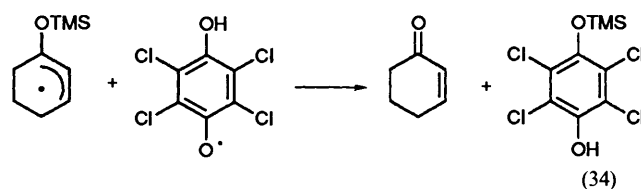
The addition of salt had the same effect on the transient species in dichloromethane as the change to a more polar solvent: the conversion of CAH[•] into CA^{•-}. Inert salt (TBA⁺ ClO₄⁻) separated the contact ion pair, eqn. (33) and thus prevented the interionic proton transfer. [There is ample precedent for the analogous suppression of proton transfer between oppositely charged ions by added salt.^{25,88}] This separation of [CA^{•-} CTE^{•+}] resulted in the persistence of the ions (CA^{•-} and CTE^{•+}) on the microsecond timescale.



CIP



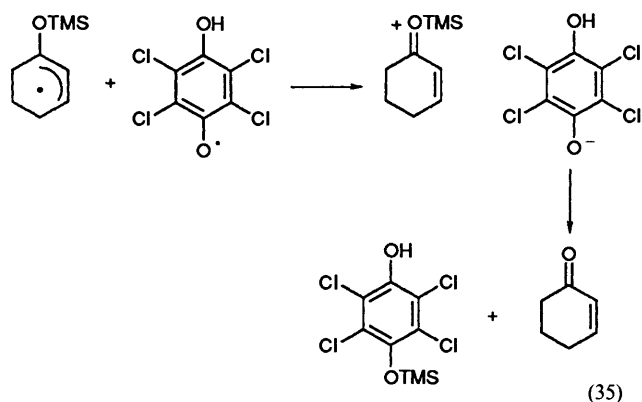
The subsequent reactions of the intermediates leading to the enone and hydroquinone derivatives (in dichloromethane) and the oxidative adduct (in acetonitrile) were followed on the microsecond timescale. The absorbance of CAH[•], monitored at 435 nm, was observed to decay in the interval 100–500 μs following the laser pulse. The decay of CAH[•] could be smoothly fitted to second-order kinetics in this interval, and the second-order rate constant (k'_{obs}) was found to be essentially invariant with the laser intensity. The apparent lifetime of CAH[•] showed a distinct decrease as the laser intensity (and thus the initial concentration of CAH[•]) was increased. The decay of CAH[•] is thus second order in photogenerated transient,⁸⁹ and the absolute rate constant for its disappearance is given by $k_2 = \epsilon k'_{\text{obs}}$, where ϵ is the molar extinction coefficient of CAH[•] at the monitoring wavelength (7700 dm³ mol⁻¹ cm⁻¹).⁸⁵ This treatment yielded a value of $k_2 = 3.7 \times 10^9 \text{ dm}^3 \text{ mol}^{-1} \text{ s}^{-1}$ for the second-order rate constant. This second-order decay can be ascribed to the radical-pair reaction of CAH[•] with the allylic radical, eqn. (34). The products of the reaction, the enone and



the trimethylsilyl ether of tetrachlorohydroquinone, were thus formed. We propose that a process of electron transfer followed by TMS⁺ transfer within the ion pair is responsible, *i.e.*, eqn. (35). This electron transfer is reasonable in view of the reduction potential of the CAH[•] radical ($E_o = 0.73 \text{ v.s. NHE}$)⁹⁰ and the facile oxidation of allylic and benzylic radicals to the carbocation.[‡]⁹¹

Kinetics of the decay of CA^{•-} in acetonitrile were complex and bimodal, consisting of partial decay (over the course of 200 μs) of the absorbance at 450 nm to a raised baseline. No further decay was observed for long (> 2 ms) times. It is likely that the distinctive oxidative adduct is formed by radical-radical coupling of CA^{•-} and the silyl ether radical cation (CTE^{•+}). [Note that radical-radical coupling of NO₂[•] with arene cation

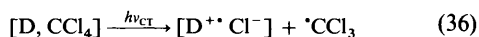
‡ In benzene, a nonpolar solvent in which the electron transfer in eqn. (35) would be less likely, an appreciable amount (30%) of aromatized product (phenyl trimethylsilyl ether) is formed *without* TMS transfer.



radicals was similarly favoured over the ion-pair annihilation process by polar solvents such as MeCN. See Section IVB.]

V. Epilogue

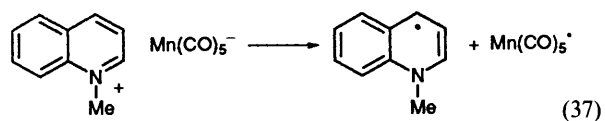
The use of time-resolved spectroscopy has enabled the full range of transient ion-pair behaviour, from the contact ion pair to the free ions, to be directly observed and quantified. The relevant lifetimes of the various ionic species range from late picoseconds to early nanoseconds for CIPs, to late nanoseconds for SSIPs, and to microseconds/milliseconds for free ions. The knowledge so gained by the quantitative time-resolved spectroscopic approach is also available for problems of photoinduced electron transfer (PET), particularly of charge-transfer activation. Further elaboration of the Winstein paradigm in the context of PET is the focus of extensive current research, and a number of details remain to be clarified. The ion-pairing behaviour of small (hard) anions such as the halides, hydroxide, or alkoxides particularly must be addressed, since these are typical leaving groups in solvolysis. The dissociative electron attachment to alkyl halides may provide one possible approach, for example, eqn. (36). Simple alkyl carbocations are not



suitable for observation by picosecond time-resolved techniques, since they do not absorb in the visible or near UV spectral regions. We hope that recent advances in time-resolved infrared and Raman spectroscopy may allow this problem to be examined. The original goal of finding a spectroscopic distinction between CIPs and SSIPs remains unfulfilled.

The three disparate ionic processes of bond formation, proton transfer and electron transfer, as described Section IV A–C are all classified within the purview of internal return, since their overall effect is to annihilate the contact ion pair. Such commonality raises the question as to whether these processes are related in some more fundamental way. Accordingly, let us consider the underlying connection as follows.

(1) Closely related ion pairs often undergo internal return by wholly different routes. For example, the *N*-methylquinolinium cation reacts with $Mn(CO)_5^-$ via electron transfer, eqn. (37), as



described in Section IVA. Under the same conditions, the structurally identical rhenium anion forms the covalent adduct, eqn. (38). A minor alteration of the cation by the substitution of hydrogen by methyl at the 4-position, diverts the reaction to proton transfer, i.e., eqn. (39).

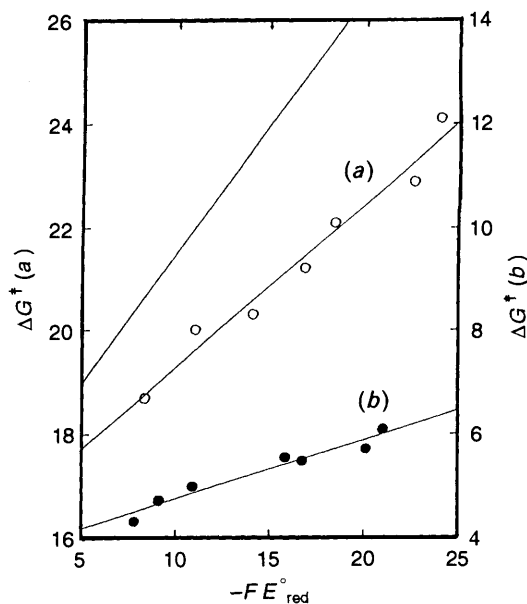
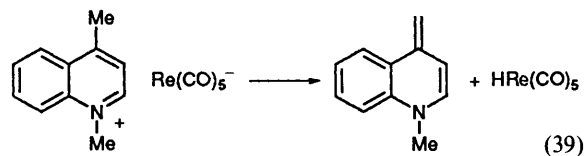
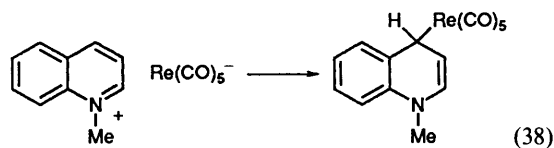


Fig. 5 Activation energy for internal return as a function of the reduction potential of the cation, as applied to (a) electron transfer within $[Py^+ Mn(CO)_5^-]$ ion pairs and (b) bond formation between anthracene cations and trinitromethanide anion. The latter values are displaced arbitrarily



Although the contact ion pairs in eqns. (37)–(39) are essentially identical in structure, their chemical fates are quite unique. We believe that this manifold reactivity of the ion pairs stems from the ambiphilic reactivity of anions as nucleophiles, as bases, and as electron donors and cations (as electrophiles, acids and electron acceptors) in internal return. The partitioning of the contact ion pair into these divergent reaction pathways will thus be the focus of further mechanistic scrutiny.

(2) The various internal-return processes respond to electronic changes in the cation and anion in similar ways. For example, the collapse of the $[A^+ T^-]$ contact ion pair correlates with the proton transfer equilibria inherent in the Hammett relation, as shown by the relatively large value of $\rho = 1.0$ for the internal return step (k_1 in Scheme 7). A more general formulation compares the ionic reactivity of cations and anions with their redox potentials, since the latter serves as a quantitative measure of electron excess. Fig. 5 shows the comparative reactivity (ΔG^\ddagger) for internal return (k_1) of (a) various pyridinium cations that react via electron transfer with $Mn(CO)_5^-$ and (b) anthracene cations that react with trinitromethanide, as plotted against the reduction potentials of the cations. Both reactions show enhanced rates (decreasing ΔG^\ddagger) as the electron deficiency of the cation is increased. The value of the slope for the interionic electron transfer is 0.31. Thus electron transfer is more sensitive to E_{red}° than bond formation (with slope 0.12), but it is less than that expected for a pure (outer-sphere) electron transfer. Other authors have pointed out the complementary correlation, between the

oxidation potentials (E_{ox}°) of anionic donors and their nucleophilic reactivity.⁹² The meaning of such linear free energy relationships, in mechanistic terms, can be considered within the framework of (i) common reactive intermediates or (ii) closely-related transition states. The nature of such intermediates or transition states will be explored.

(3) Electron-deficient cations and electron-rich anions are *acceptors* and *donors*, respectively, according to the Mulliken formulation. Internal return thus constitutes a donor-acceptor combination, with the contact ion pair serving as the precursor EDA complex. Our studies of the charge-transfer interaction between *neutral* substrates have identified the EDA complex as the critical precursor in aromatic substitutions, cycloadditions and cycloreversions, electron transfers, oxygenations and hydrogenations.^{93,94} In each case, the complex can be identified by its characteristic charge-transfer (CT) electronic absorption bands. The validity of this formulation for *ion pairs* is demonstrated by the CT bands of $[\text{Py}^+\text{Mn}(\text{CO})_5^-]$ and related contact ion pairs in Section IVA. The charge-transfer absorption bands of the contact ion pair directly reflect the electronic overlap between cationic acceptor and anionic donor. Since this overlap must precede any of the various collapse processes, the solution to the problem of differing reactivities of the CIP must therefore lie in an understanding of the formation, energies and spectral behaviour of charge-transfer bands.

There has been considerable theoretical exploration of the connection between nucleophile-electrophile, acid-base and donor-acceptor interactions. These various formulations have not been easy to test, however, and it remains to be clarified as to what sort of framework is needed to unify all these diverse and apparently distinctive reactions. We believe that the *experimental* groundwork for the solution to this problem will come from the direct observation of internal return on the (femtosecond) timescale appropriate to bond-making and -breaking, and electron and proton transfer. The once-forbidding technical problem of the generation of ultrashort femtosecond laser pulses is already being solved, and it is now possible to generate the reactive intermediates. The solution to the mechanistic problems of the relationship between various internal return processes thus lies in the design of chemical systems to elicit the needed information.

Experimental

Materials

Tetrachloro-*p*-benzoquinone (chloranil, Aldrich) was sublimed *in vacuo* and recrystallized from benzene. Cyclohex-1-enyl trimethylsilyl ether (CTE) and (2-methylcyclohex-1-enyl) trimethylsilyl ether were prepared by the method of Cazeau *et al.*⁹⁵ (6-Methylcyclohex-1-enyl) trimethylsilyl ether was prepared as described by Fleming and Paterson.⁹⁶ Hexamethyldisilane and cyclohexa-1,3-diene (Aldrich) were distilled before use. The *N*-methylpyridinium triflates were prepared from the pyridine bases and methyl triflate.^{11b} The PPN^+ salt of pentacarbonylmanganate was prepared as described in ref. 59.

Dichloromethane (Mallinckrodt, reagent) was repeatedly stirred with fresh aliquots of conc. sulfuric acid until the acid layer remained colourless. It was then washed successively with water and aqueous sodium hydrogen carbonate, and dried with anhydrous calcium chloride. It was initially distilled from phosphorus pentoxide, and then redistilled from calcium hydride under an inert atmosphere of argon. Acetonitrile (Fischer, reagent) was stirred with potassium permanganate (0.1% by weight) for a day, and the mixture was refluxed until colourless. After removal of MnO_2 by decantation, the acetonitrile was distilled from phosphorus pentoxide. It was

then redistilled from calcium hydride. Tetrahydrofuran was distilled from lithium aluminium hydride. The solvents were stored in Schlenk flasks under an atmosphere of argon.

Instrumentation

Electronic absorption spectra were recorded on a Hewlett-Packard 8450-A diode-array spectrometer with 2 nm resolution. ^1H NMR spectra were measured in $[\text{H}]$ chloroform or $[\text{H}_3]$ acetonitrile on a General Electric QE 300 FT spectrometer. Infrared spectra were recorded on a Nicolet 10-DX FT-IR spectrometer. Gas chromatographic analyses were performed on a Hewlett-Packard 5890 gas chromatograph with 12.5 m cross-linked dimethylsilicone capillary column. GC-MS measurements were carried out on a Hewlett-Packard 5890A chromatograph interfaced to an HP 5970 mass spectrometer (70 eV, EI). High performance liquid chromatography (HPLC) employed an LDC Analytical model 3000 equipped with dual pumps (constaMetric 3200 and 3500 solvent delivery systems) and a UV detector (spectroMonitor 3100). Analytical HPLC was carried out with a reversed-phase column (Hypersil BDC C_{18} 5 μ). The mobile-phase solvents were 5% methanolic water (distilled) and HPLC grade acetonitrile. Integration of the signals was carried out with a Hewlett-Packard 3394A integrator.

Steady-state photochemical experiments utilized a focussed beam from either a 500 W Osram (HBO-212) high-pressure Hg lamp or an 450 W Osram (XBO-500 W/H) xenon lamp. The beam was passed through an IR (water) filter coupled to the appropriate sharp cut-off filter (Corning CS series) and then onto a Pyrex Schlenk cuvette immersed in a water bath.

The laser source for the *picosecond* time-resolved diffuse reflectance measurements was a mode-locked Nd:YAG laser (Quantel, YG501-C) with a 30 ps pulse. Both the harmonic (355 or 532 nm) and the fundamental (1064 nm) light pulse were extracted from the laser. The harmonic laser beam traversed a variable (up to 5 ns) delay stage before being directed onto the sample cuvette as excitation beam. The fundamental laser light was focussed onto a 10 cm cuvette containing a 50:50 mixture of D_2O and H_2O to produce a white continuum flash of 25 ps duration which was then collimated to a narrow beam and split into two directions by means of a neutral density filter as semi-transparent mirror. One beam was directly picked up by fibre optics (reference beam), the other beam was directed onto the sample cuvette overlapping with the excitation beam in order to probe the excited sample. A portion of the diffuse reflected white light was picked up by a second fibre optic mounted at an angle very close to the cuvette surface and equipped with an appropriate cut-off filter in front of the aperture to reduce scattered light from the excitation pulse. The two optical fibres led to an Instrument S.A. flat-field spectrograph (HR320) to which an unintensified dual-diode array detector (Princeton Instruments, DDA-512) was attached. Thus, with each laser shot two spectra (excited sample and reference) could be detected simultaneously. In a typical experiment 100 spectra were averaged. Before each measurement the reference and sample light beams were balanced and all data were corrected by this balance. The diode array signals were passed to a personal computer *via* a Princeton Instruments interface for data storage, display and analysis.

The *nanosecond* time-resolved diffuse-reflectance measurements were performed using a Q-switched Nd:YAG laser (Quantel, YG 580-10) and a kinetic spectrometer consisting of an Oriel 150 W xenon lamp, an Oriel monochromator, a Hamamatsu photomultiplier tube (R 928), and a Tektronix oscilloscope (7104) equipped with a digital camera (CI001). Data acquisition was controlled by a sequence generator, laser controller, and back-off unit from Kinetics Instruments. The

data were fed into a personal computer for storage and analysis using programs written in ASYST.

Steady-state Photoreactions of Chloranil with Enol Silyl Ethers

In a typical experiment a solution of 0.04 mol dm⁻³ chloranil and 0.04 mol dm⁻³ silyl ether in 5.0 cm³ dichloromethane or acetonitrile were irradiated with the focussed beam from the 500 W Hg lamp. When the pale red solution was bleached (1 h) an aliquot (0.5 cm³) of the reaction mixture was removed for GC and HPLC analysis, and the remainder of the solution was evaporated *in vacuo*. The solvent was replaced with [²H]-chloroform and 1,2-dichloroethane was added as an internal standard for ¹H NMR analysis. The adduct, [*O*-(2-oxocyclohexyl)tetrachloro-1,4-hydroquinonyl trimethylsilyl ether] was quantified using the characteristic resonance of δ 4.77. The yield of the mono-trimethylsilyl ether of tetrachlorohydroquinone was determined from its resonance at δ 0.23. The yield of cyclohexenone was determined by GC and GC-MS using tetradecane as the internal standard.

The desilylated adduct was isolated from the photolysed acetonitrile solution by column chromatography on silica gel using a 95:5 (v:v) mixture of hexanes and ethyl acetate as the eluent. The product formed colourless microcrystals. δ_{H} (300 MHz; [²H₃]acetonitrile) 4.77 (1 H, dd, $J = 10.6, 4.6$ Hz), 2.45 (m, 2 H), 2.23 (m, 2 H), 1.90 (m, 2 H) and 1.69 (m, 2 H). [The desilylated DDQ analogue⁷⁷ had δ 5.11 (dd, $J = 10.7, 5.9$ Hz).] GC-MS analysis of the crude photolysate showed that the adduct was silylated ($M^+ = 410, 412, 414, 416$ for C₁₅H₁₈Cl₄O₃Si). Since the ¹H NMR spectrum of the isolated adduct showed no resonances at $\delta < 1.5$, it was concluded that desilylation occurred during chromatographic work-up.

Appendix

Let c be the initial concentrations of PPN⁺ Mn(CO)₅⁻ and Py⁺ OTf⁻. Then $[\text{Py}^+ \text{OTf}^-] = [\text{PPN}^+ \text{Mn}(\text{CO})_5^-] = c - \xi - [\text{Py}^+ \text{Mn}(\text{CO})_5^-]$, and $[\text{PPN}^+ \text{OTf}^-] = \xi + [\text{Py}^+ \text{OTf}^-]$. The ion-pair equilibrium in Scheme 9 therefore implies that $\{c - \xi - [\text{Py}^+ \text{Mn}(\text{CO})_5^-]\}^2 = K_x [\text{Py}^+ \text{Mn}(\text{CO})_5^-] \{\xi + [\text{Py}^+ \text{Mn}(\text{CO})_5^-]\}$. Since $K_x = 1$ then $[\text{Py}^+ \text{Mn}(\text{CO})_5^-] = (c - \xi)^2 / (2c - \xi)$. The differential equation for the kinetics then becomes $d\xi/dt = k_{\text{et}}[\text{Py}^+ \text{Mn}(\text{CO})_5^-] = k_{\text{et}}(c - \xi)^2 / (2c - \xi)$. After separation of the variables and integration, eqn. (19) is obtained. During the first phase of the reaction, when ξ is small relative to c , the second term in eqn. (19) is approximated by $\ln [c/(c - \xi)]$ and the equation reduces to $\ln [c/(c - \xi)] = 1/2 k_{\text{et}}t$ for first-order kinetics. In the presence of a large concentration (c_s) of added salt, the logarithmic term in eqn. (20) is insignificant, and the expression for second-order kinetics, $\xi/(c - \xi) = k't$ obtains, where $k' = [c/(c + c_s)]k_{\text{et}}$.

Acknowledgements

We thank our colleagues, especially John M. Masnovi and S. Sankararaman, for their tireless effort and creative ideas. In addition we thank the National Science Foundation, the Welch Foundation and the Texas Advanced Research Program for financial support.

References

- (a) H. Sadek and R. M. Fuoss, *J. Am. Chem. Soc.*, 1954, **76**, 5897, 5905; (b) R. M. Fuoss and F. Accascina, *Electrolytic Conductance*, Wiley, New York, 1959.
- S. Winstein, E. Clippinger, A. H. Fainberg and G. C. Robinson, *J. Am. Chem. Soc.*, 1954, **76**, 2597.
- (a) *Ions and Ion Pairs in Organic Reactions*, ed. M. Szwarc, Vols. I and II, Wiley, New York, 1972, 1974; (b) J. E. Gordon, *Organic Chemistry of Electrolyte Solutions*, Wiley, New York, 1975.
- W. F. Edgell in ref. 3(a).
- H. Hirota and S. I. Weissman, *J. Am. Chem. Soc.*, 1964, **86**, 2538.
- (a) E. H. Cordes and R. B. Dunlap, *Acc. Chem. Res.*, 1969, **2**, 329; (b) H. Kessler and M. Feigel, *Acc. Chem. Res.*, 1982, **15**, 2.
- (a) G. Atkinson and S. Petrucci, *J. Phys. Chem.*, 1966, **70**, 2550, 3122; (b) A. Fanelli and S. Petrucci, *J. Phys. Chem.*, 1971, **74**, 2649; (c) J. Stuer in *Investigation of Rates and Mechanisms of Reactions, Part II*, ed. G. G. Hammes, Wiley, New York, 1974, p. 237 ff.
- (a) T. E. Hogen-Esch and J. Smid, *J. Am. Chem. Soc.*, 1966, **88**, 307; (b) T. E. Hogen-Esch, *Adv. Phys. Org. Chem.*, 1977, **15**, 153.
- (a) W. F. Edgell, J. Lyford, A. Barbetta and C. I. Jose, *J. Am. Chem. Soc.*, 1971, **93**, 6403; (b) W. F. Edgell, S. Hegde and A. Barbetta, *J. Am. Chem. Soc.*, 1978, **100**, 1406; (c) M. Y. Darensbourg, *Prog. Inorg. Chem.*, 1985, **13**, 221.
- (a) E. M. Kosower, *J. Am. Chem. Soc.*, 1958, **80**, 3253; (b) E. M. Kosower and J. A. Skorcz, *J. Am. Chem. Soc.*, 1960, **82**, 2195; (c) E. M. Kosower and M. Mohammad, *J. Phys. Chem.*, 1970, **74**, 1153.
- (a) T. M. Bockman and J. K. Kochi, *J. Am. Chem. Soc.*, 1989, **111**, 4669; (b) T. M. Bockman and J. K. Kochi, *New J. Chem.*, 1992, **16**, 39; (c) T. M. Bockman, H.-R. Chang, H. G. Drickamer and J. K. Kochi, *J. Phys. Chem.*, 1990, **94**, 8483.
- (a) S. Goldman and G. C. B. Cave, *Can. J. Chem.*, 1971, **49**, 1726; (b) L. D. Pettit and S. Bruckenstein, *J. Am. Chem. Soc.*, 1966, **88**, 4783.
- C. F. Bernasconi, *Investigation of Rates and Mechanisms of Reactions Part I*, ed. C. F. Bernasconi, Wiley, New York, 1986, p. 426 ff.
- Ref. 3 (b), p. 508 ff.
- (a) M. Eigen and J. Johnson, *Ann. Rev. Phys. Chem.*, 1960, **11**, 307; (b) G. G. Hammes, *Ann. Rev. Phys. Chem.*, 1964, **15**, 13; (c) G. Schwarz, *Rev. Mod. Phys.*, 1968, **40**, 206.
- (a) H. Strehlow, *Fast Reactions in Solution*, Blackwell, Oxford, 1964; (b) G. Czlerinski, *Chemical Relaxation*, Dekker, New York, 1966.
- (a) E. F. Hilinski and P. M. Rentzepis, *Acc. Chem. Res.*, 1983, **16**, 224; (b) N. Mataga, *Pure Appl. Chem.*, 1984, **56**, 1255; (c) B. I. Green, R. M. Hochstrasser and R. B. Weisman, *J. Chem. Phys.*, 1979, **70**, 1247; (d) S. M. Hubig and M. A. J. Rodgers in *Handbook of Organic Photochemistry, Vol I*, ed. J. C. Scaiano, CRC Press, Boca Raton, FL, 1989, p. 315 ff.
- (a) C. V. Shank, *Science*, 1983, **219**, 1027; (b) M. R. Wasielewski, M. P. Niemczyk, W. A. Svec and E. B. Pewett, *J. Am. Chem. Soc.*, 1985, **107**, 5562; (c) T. Asahi and N. Mataga, *J. Phys. Chem.*, 1991, **95**, 1956; (d) C. A. Langhoff, K. Gnädig and K. B. Eisenthal, *Chem. Phys.*, 1980, **46**, 117; (e) A. L. Harris, M. Berg and C. B. Harris, *J. Chem. Phys.*, 1986, **84**, 788.
- (a) M. R. Wasielewski and D. M. Tiede, *FEBS Lett.*, 1986, **204**, 368; (b) N. W. Woodbury, M. Becker, D. Middendorf and W. W. Parson, *Biochemistry*, 1985, **24**, 7516; (c) E. F. Hilinski, J. M. Masnovi, C. Amatore, J. K. Kochi and P. M. Rentzepis, *J. Am. Chem. Soc.*, 1983, **106**, 6167.
- (a) J. J. Cosa and H. E. Gspöner, *J. Photochem. Photobiol. A*, 1989, **303**; (b) G. Jones, II and K. Goswami, *J. Phys. Chem.*, 1986, **90**, 5414.
- K. G. Spears, T. H. Gray and D. Huang, *J. Phys. Chem.*, 1986, **90**, 779.
- (a) L. E. Manring and K. S. Peters, *J. Phys. Chem.*, 1984, **88**, 3516; (b) K. S. Peters and B. Li, *J. Phys. Chem.*, 1994, **98**, 401.
- (a) R. A. McClelland, V. M. Kanagasabapathy, N. S. Banait and S. Steenken, *J. Am. Chem. Soc.*, 1991, **113**, 1009; (b) F. L. Cozens, N. Mathivanan, R. A. McClelland and S. Steenken, *J. Chem. Soc., Perkin Trans. 2*, 1992, 2083.
- G. J. Kavarnos and N. J. Turro, *Chem. Rev.*, 1986, **86**, 401.
- (a) J. D. Simon and K. S. Peters, *J. Am. Chem. Soc.*, 1981, **103**, 6403; (b) J. D. Simon and K. S. Peters, *J. Am. Chem. Soc.*, 1982, **104**, 6142, 6542; (c) J. S. Simon and K. S. Peters, *J. Am. Chem. Soc.*, 1983, **105**, 4879.
- C. Devadoss and R. W. Fessenden, *J. Phys. Chem.*, 1990, **94**, 4540.
- H. Miyasaka, K. Morita, K. Kamada and N. Mataga, *Chem. Phys. Lett.*, 1991, **178**, 504.
- (a) E. Haselbach, E. Vauthey and P. Suppan, *Tetrahedron*, 1988, **44**, 7335; (b) E. Haselbach, P. Jaques, D. Pilloud, P. Suppan and E. Vauthey, *J. Phys. Chem.*, 1991, **95**, 7115.
- (a) J. Gersdorf and J. Mattay, *J. Photochem.*, 1985, **28**, 403; (b) J. Gersdorf, J. Mattay and H. Görner, *J. Am. Chem. Soc.*, 1987, **109**, 1203.
- (a) E. F. Hilinski, S. V. Milton and P. M. Rentzepis, *J. Am. Chem. Soc.*, 1983, **105**, 5193; (b) J. P. Sournillion, P. Vandereecken, M. Van Der Auweraer, F. C. De Schryver and A. Schank, *J. Am. Chem. Soc.*, 1987, **109**, 2217.

- 31 K. I. Zamaraev and R. F. Khairutdinov, *Top. Curr. Chem.*, 1992, **163**, 4.
- 32 R. M. Noyes, *Prog. React. Kinet.*, 1961, **1**, 129.
- 33 Yu. N. Molin, ed., *Spin Polarization and Magnetic Effects in Radical Reactions*, Elsevier, New York, 1984.
- 34 (a) H. D. Roth and M. L. M. Schilling, *J. Am. Chem. Soc.*, 1980, **102**, 4303; (b) R. Kaptein *Adv. Free Radical Chem.*, 1975, **5**, 319.
- 35 K. S. Peters and J. Lee, *J. Phys. Chem.*, 1993, **97**, 3761.
- 36 H. Miyasaka, K. Morita, K. Kamada and N. Mataga, *Bull. Chem. Soc. Jpn.*, 1990, **63**, 3385.
- 37 (a) R. S. Mulliken, *J. Am. Chem. Soc.*, 1952, **74**, 811; (b) L. E. Orgel and R. S. Mulliken, *J. Am. Chem. Soc.*, 1957, **79**, 4839.
- 38 E. F. Hilinski, J. M. Masnovi, C. Amatore, J. K. Kochi and P. M. Rentzepis, *J. Am. Chem. Soc.*, 1983, **105**, 6167.
- 39 N. Mataga, *Pure Appl. Chem.*, 1993, **65**, 1605.
- 40 J. M. Masnovi and J. K. Kochi, *J. Am. Chem. Soc.*, 1985, **107**, 7880.
- 41 J. M. Masnovi, J. K. Kochi, E. F. Hilinski and P. M. Rentzepis, *J. Am. Chem. Soc.*, 1986, **108**, 1126.
- 42 (a) S. Sankararaman, W. A. Haney and J. K. Kochi, *J. Am. Chem. Soc.*, 1987, **109**, 5235; (b) S. Sankararaman, W. A. Haney and J. K. Kochi, *J. Am. Chem. Soc.*, 1987, **109**, 7824.
- 43 J. M. Masnovi and J. K. Kochi, *J. Am. Chem. Soc.*, 1985, **107**, 6781.
- 44 T. Yabe and J. K. Kochi, *J. Am. Chem. Soc.*, 1992, **114**, 4491.
- 45 J. M. Masnovi, E. A. Seddon and J. K. Kochi, *Can. J. Chem.*, 1984, **62**, 2552.
- 46 J. Mattay and M. Vondenhof, *Top. Curr. Chem.*, 1991, **159**, 219.
- 47 S. Winstein and A. H. Fainberg, *J. Am. Chem. Soc.*, 1958, **80**, 459.
- 48 S. Winstein and D. Trifan, *J. Am. Chem. Soc.*, 1956, **78**, 2784.
- 49 See ref. 3(b), p. 389.
- 50 (a) E. M. Arnett, E. B. Troughton and K. E. Molter, *J. Am. Chem. Soc.*, 1984, **106**, 6726; (b) E. M. Arnett, S. Venimadhaven and K. Amarnath, *J. Am. Chem. Soc.*, 1992, **114**, 5598; (c) E. M. Arnett and R. A. Flowers, II, *Chem. Soc. Rev.*, 1993, 9.
- 51 (a) F. G. Bordwell and J. P. Chang, *J. Am. Chem. Soc.*, 1991, **113**, 1736; (b) F. G. Bordwell and H. J. Bausch, *J. Am. Chem. Soc.*, 1986, **108**, 1979.
- 52 J.-M. Savéant, *Acc. Chem. Res.*, 1993, **26**, 455.
- 53 (a) J. M. Harris, *Prog. Phys. Org. Chem.*, 1974, **11**, 89; (b) T. W. Bentley and P. von R. Schleyer, *Adv. Phys. Org. Chem.*, 1977, **14**, 1; (c) D. J. Raber, J. M. Harris and P. von R. Schleyer, in ref. 3(a), Vol II, p. 247.
- 54 (a) R. A. Sneen and J. W. Larsen, *J. Am. Chem. Soc.*, 1969, **91**, 6031; (b) R. A. Sneen, *Acc. Chem. Res.*, 1973, **6**, 46.
- 55 (a) A. Williams, *Adv. Phys. Org. Chem.*, 1992, **27**, 1; (b) A. D. Allen, V. M. Kanagsabapathy and T. T. Tidwell, in *Nucleophilicity*, eds. J. M. Harris and S. P. McManus, ACS, Washington, 1987, p. 315.
- 56 (a) D. J. Kuchynka, C. A. Amatore and J. K. Kochi, *J. Organomet. Chem.*, 1987, **328**, 133; (b) C.-K. Lai, W. G. Feighery, Y. Zhen and J. D. Atwood, *Inorg. Chem.*, 1989, **28**, 3929.
- 57 M. Tilset and V. D. Parker, *J. Am. Chem. Soc.*, 1989, **111**, 6711.
- 58 E. M. Kosower and J. A. Skorcz, *J. Am. Chem. Soc.*, 1960, **82**, 2195.
- 59 R. A. Faltynek and M. S. Wrighton, *J. Am. Chem. Soc.*, 1978, **100**, 2701.
- 60 P. S. Braterman, *Metal Carbonyl Spectra*, Academic, New York, 1975, p. 193.
- 61 A. K. Colter, C. C. Lai, A. G. Parsons, N. B. Ramsey and G. Saito, *Can. J. Chem.*, 1985, **63**, 445.
- 62 A. Anne, P. Hapiot, J. Moireux, P. Neta and J.-M. Saveant, *J. Am. Chem. Soc.*, 1992, **114**, 4694.
- 63 T. R. Herrinton and T. L. Brown, *J. Am. Chem. Soc.*, 1985, **107**, 5700.
- 64 M. Darsenbourg, H. Barros and C. Borman, *J. Am. Chem. Soc.*, 1977, **99**, 1647.
- 65 J. A. Dean, ed., *Lange's Handbook of Chemistry*, 12th edn., McGraw-Hill, New York, 1979.
- 66 S. Winstein and E. Clippinger, *J. Am. Chem. Soc.*, 1956, **78**, 2784.
- 67 J. K. Kochi, in *Comprehensive Organic Syntheses*, Vol VII, ed. B. M. Trost, Pergamon, New York, 1991, p. 849.
- 68 E. Heilbronner, *Helv. Chim. Acta*, 1953, **36**, 1121.
- 69 E. K. Kim, T. M. Bockman and J. K. Kochi, *J. Chem. Soc., Perkin Trans. 2*, 1992, 1879.
- 70 E. K. Kim, T. M. Bockman and J. K. Kochi, *J. Am. Chem. Soc.*, 1993, **115**, 3091.
- 71 M. A. Fox and M. Chanon, *Photoinduced Electron Transfer*, Elsevier, Amsterdam, 1988.
- 72 (a) J. Mattay, *Synthesis*, 1989, 233; (b) J. Mattay, *Angew. Chem., Int. Ed. Engl.*, 1987, **26**, 825.
- 73 A. Loupy and B. Tchoubar, *Salt Effects in Organic and Organometallic Chemistry*, VCH, New York, 1992, p. 232 ff.
- 74 J. Goodman and K. S. Peters, *J. Am. Chem. Soc.*, 1985, **107**, 6409.
- 75 S. Perrier, T. M. Bockman and J. K. Kochi, *J. Chem. Soc., Perkin Trans. 2*, 1993, 595.
- 76 D. Knausz, A. Mesztyczky, L. Szakacs, B. Csakvari and K. Ujszaszy, *J. Organomet. Chem.*, 1983, **256**, 11.
- 77 A. Bhattacharya, L. M. DiMichele, U. H. Dolling, E. J. J. Grabowski and V. J. Grenda, *J. Org. Chem.*, 1989, **54**, 6118.
- 78 (a) R. Rathore, unpublished results; (b) S. L. Murov, I. Carmichael and G. L. Hug, *Handbook of Photochemistry*, 2nd edn., Dekker, New York, 1993, p. 261; (c) K. B. Petrushenko, A. I. Vokin, V. K. Turchaninov, A. G. Gorshkov and Yu. L. Frolov, *Isv. Akad. Nauk SSSR, Ser. Khim. (Engl. Transl.)*, 1985, **34**, 242; (d) H. Kobashi, H. Gyoda and T. Morita, *Bull. Chem. Soc. Jpn.*, 1977, **50**, 1731.
- 79 (a) R. Gschwind and E. Haselbach, *Helv. Chim. Acta*, 1979, **62**, 941; (b) E. Guerry-Butty, E. Haselbach, C. Pasquier, P. Suppan and D. Phillips, *Helv. Chim. Acta*, 1985, **68**, 912.
- 80 (a) P. M. Rentzepis, D. W. Steyert, H. D. Roth and C. J. Abelt, *J. Phys. Chem.*, 1985, **89**, 3955; (b) E. F. Hilinski and P. M. Rentzepis, *J. Am. Chem. Soc.*, 1983, **105**, 5193.
- 81 (a) G. Jones, II and W. A. Haney, *J. Phys. Chem.*, 1986, **90**, 5410; (b) G. Jones, II and N. Mouli, *J. Phys. Chem.*, 1988, **92**, 7174.
- 82 (a) P. P. Levin, P. F. Pluznikov and V. A. Kuzmin, *Chem. Phys. Lett.*, 1988, **147**, 283; (b) V. A. Kuzmin and P. P. Levin, *Isv. Akad. Nauk SSSR Ser. Khim. (Engl. Transl.)*, 1988, 429.
- 83 (a) D. R. Kemp and G. Porter, *J. Chem. Soc. D*, 1969, 1029; (b) K. Kawai, Y. Shiota, T. Tsubomura and H. Mikawa, *Bull. Chem. Soc. Jpn.*, 1972, **45**, 77.
- 84 J. J. Andre and G. Weill, *Mol. Phys.*, 1968, **15**, 97.
- 85 S. K. Wong, L. Fabes, W. J. Green and J. K. S. Wan, *J. Chem. Soc., Faraday Trans. 1*, 1972, **68**, 2211.
- 86 cf. J. H. Ridd, *Adv. Phys. Org. Chem.*, 1979, **16**, 1.
- 87 cf. M. T. Crow, A. Alberti, C. M. Depew and J. K. S. Wan, *Bull. Chem. Soc. Jpn.*, 1985, **58**, 3675.
- 88 (a) Y. Hayashi and T. Mukaiyama, *Chem. Lett.*, 1987, 1811; (b) R. Corriu and J. Guenzat, *Tetrahedron Lett.*, 1968, 6083; (c) H. Strzelecka, *C. R. Acad. Sci., Ser. C*, 1972, **275**, 617; (d) Y. Pocker and J. C. Ciula, *J. Am. Chem. Soc.*, 1988, **110**, 2904.
- 89 J. W. Moore and R. G. Pearson, *Kinetics and Mechanism*, 3rd edn., Wiley, New York, 1981, p. 160.
- 90 P. R. Rich and D. S. Bendall, *Biochem. Biophys. Acta*, 1980, **592**, 506.
- 91 C. J. Schlesener, C. Amatore and J. K. Kochi, *J. Am. Chem. Soc.*, 1984, **106**, 3567.
- 92 (a) R. E. Dessy, R. L. Pohl and R. B. King, *J. Am. Chem. Soc.*, 1966, **88**, 5121; (b) F. G. Bordwell and M. J. Bausch, *J. Am. Chem. Soc.*, 1986, **108**, 1979.
- 93 J. K. Kochi, *Adv. Phys. Org. Chem.*, 1994, **29**, 185.
- 94 (a) K. Brüggerman, R. S. Czernuszewicz and J. K. Kochi, *J. Phys. Chem.*, 1992, **96**, 4405; (b) K. Brüggerman and J. K. Kochi, *J. Org. Chem.*, 1992, **57**, 2956; (c) J. J. Ko, T. M. Bockman and J. K. Kochi, *Organometallics*, 1990, **9**, 1833; (d) J. K. Kochi, *Chimia*, 1991, **45**, 277; (e) R. E. Lehmann and J. K. Kochi, *J. Am. Chem. Soc.* 1991, **113**, 501.
- 95 P. Cazeau, F. Duboudin, F. Moulines, O. Babot and J. Dunogues, *Tetrahedron*, 1987, **43**, 2075.
- 96 I. Paterson and I. Fleming, *Synthesis*, 1979, 736.